Behavioral/Cognitive

Processing of Hedonic and Chemosensory Features of Taste in Medial Prefrontal and Insular Networks

Ahmad Jezzini,* Luca Mazzucato,* Giancarlo La Camera, and Alfredo Fontanini

Department of Neurobiology and Behavior and Graduate Program in Neuroscience, State University of New York at Stony Brook, Stony Brook, New York 11794

Most of the research on cortical processing of taste has focused on either the primary gustatory cortex (GC) or the orbitofrontal cortex (OFC). However, these are not the only areas involved in taste processing. Gustatory information can also reach another frontal region, the medial prefrontal cortex (mPFC), via direct projections from GC. mPFC has been studied extensively in relation to its role in controlling goal-directed action and reward-guided behaviors, yet very little is known about its involvement in taste coding. The experiments presented here address this important point and test whether neurons in mPFC can significantly process the physiochemical and hedonic dimensions of taste. Spiking responses to intraorally delivered tastants were recorded from rats implanted with bundles of electrodes in mPFC and GC. Analysis of single-neuron and ensemble activity revealed similarities and differences between the two areas. Neurons in mPFC can encode the chemosensory identity of gustatory stimuli. However, responses in mPFC are sparser, more narrowly tuned, and have a later onset than in GC. Although taste quality is more robustly represented in GC, taste palatability is coded equally well in the two areas. Additional analysis of responses in neurons processing the hedonic value of taste revealed differences between the two areas in temporal dynamics and sensitivities to palatability. These results add mPFC to the network of areas involved in processing gustatory stimuli and demonstrate significant differences in taste-coding between GC and mPFC.

Introduction

The insular cortex is the main cortical recipient of gustatory information. Ascending inputs carrying taste-related signals reach the gustatory portion of the insular cortex (GC) from subcortical relays (Spector and Travers, 2005; Carleton et al., 2010). Neurons in GC integrate information from multiple gustatory afferents and generate dynamic and multimodal responses known to encode the physiochemical and psychological dimensions of taste (Katz et al., 2002; Fontanini and Katz, 2008; Jezzini et al., 2012; Maffei et al., 2012; Piette et al., 2012; Samuelsen et al., 2012). However, the gustatory cortex (GC) is not the only cortical area involved in processing taste. GC sends projections capable of carrying gustatory information to two frontal areas: the orbitofrontal cortex (OFC) (Baylis et al., 1995; Gutierrez et al., 2006) and the medial prefrontal cortex (mPFC) (Gabbott et al., 2003).

Although a considerable amount of work has been devoted to studying how OFC processes gustatory stimuli (Kadohisa et al., 2005; Gutierrez et al., 2006, 2010; Small et al., 2007), the role of mPFC in taste is much less understood. In mammals, the mPFC has been studied mostly in reference to its function in controlling goal-directed actions and reward-guided behaviors (Matsumoto et al., 2003; Wallis and Kennerley, 2010; Laubach, 2011; Kvitsiani et al., 2013). In these experimental conditions, neurons in mPFC respond to rewarding or aversive outcomes (Baeg et al., 2001; Zhang et al., 2004; Horst and Laubach, 2013). Neurons in mPFC can encode different type of rewards (i.e., sucrose, juice, intracranial stimulation; Takenouchi et al., 1999; Amiez et al., 2006; Petykó et al., 2009), and the magnitude of their responses correlates with the magnitude of the reward (Amiez et al., 2006). In addition, mPFC neurons display characteristic patterns of persistent firing with outcome- and task-dependent changes in firing rates that can be maintained for several seconds (Baeg et al., 2001, 2003; Narayanan and Laubach, 2008, 2009).

What is known about how mPFC encodes taste comes from experiments relying on complex behavioral tasks using sucrose or juice as rewards. To our knowledge, no study has directly investigated how mPFC represents the chemosensory and hedonic dimensions of different tasting solutions. Given the strong inputs from GC (Gabbott et al., 2003), it is reasonable to expect that neurons in mPFC might encode not only reward value but also chemosensory identity. The connectivity of these two areas also suggests that gustatory information may reach mPFC only after having been processed in GC. However, the lack of data from combined recordings of mPFC and GC in a paradigm optimized to study sensory processing has made it difficult to compare gustatory dynamics in the two areas.

The experiments conducted in this study were designed to directly address how mPFC processes gustatory information and

Received July 12, 2013; revised Oct. 18, 2013; accepted Oct. 24, 2013.

Author contributions: A.J. and A.F. designed research; A.J. performed research; A.J., L.M., G.L.C., and A.F. analyzed data; A.J., L.M., G.L.C., and A.F. wrote the paper.

This work was supported by National institute of Deafness and Other Communication Disorders Grant R01-DC010389 and by a Klingenstein Foundation Fellowship (A.F.). We thank Dr. Arianna Maffei for insightful comments and Amy Chung for help with histological procedures.

*A.J. and L.M. contributed equally to this manuscript.

The authors declare no competing financial interest.

Correspondence should be addressed to Alfredo Fontanini, Department of Neurobiology and Behavior, Life Science Building, Room 545, State University of New York at Stony Brook, Stony Brook, NY 11794. E-mail: alfredo.fontanini@stonybrook.edu.

DOI:10.1523/JNEUROSCI.2974-13.2013

 0270-6474/13/3318966-13$15.00/0

how taste-evoked dynamics in mPFC relate to GC activity. By relying on the passive delivery of tasting solutions while recording neural ensembles in mPFC and GC, our experiments allowed us to investigate neural responses to taste in isolation of cognitive influences. We found that neurons in mPFC can sequentially encode both the identity and the palatability of gustatory stimuli and that response properties and dynamics differed from those observed in GC. The results provide a novel description of the involvement of mPFC in taste coding and demonstrate significant functional differences between GC and mPFC.

Materials and Methods

Experimental subjects. The experiments of this study were performed on eight female Long–Evans rats (250–350 g). Animals were maintained on a 12 h light/dark cycle with *ad libitum* food and water diet, unless otherwise specified. All experimental protocols were approved by the Institutional Animal Care and Use Committee of Stony Brook University and complied with university, state, and federal regulations on the care and use of laboratory animals.

Surgery. Stereotactic surgeries were performed under aseptic conditions and general anesthesia (ketamine–xylazine–acepromazine mixture at 100, 5.2, and 1 mg/kg, respectively). Two movable electrode bundles were implanted unilaterally in the GC (AP, 1.4 mm; ML, 5 mm from bregma; DV, 4.5 mm from the dura) and in the mPFC (AP, 3.2 mm; ML, 0.7 mm; DV, 2.5 mm from the dura). To allow gustatory stimuli delivery, intraoral cannulae (IOCs) were implanted bilaterally (Phillips and Norgren, 1970). A 7 d postsurgical recovery period was given to each animal. Pain and antibiotic medications were administered during the recovery period.

Gustatory stimulation. After recovery from surgical procedures, rats were placed on a water restriction regimen (45 min of water access per day). Subjects were habituated to stay calmly in a behavioral box and to receive and drink fluids through the IOCs. During each recording session, four basic tastants [0.1 M sucrose (S), 0.1 M sodium chloride (N), 0.2 M citric acid (C), and 0.001 M quinine (Q)] were delivered directly into the mouth through the IOC by means of a manifold of four polyimide tubes (Samuelsen et al., 2013). The concentrations used for the four tastants are consistent with the ranges reported in the literature (Yamamoto et al., 1985; Verhagen et al., 2003; Fontanini and Katz, 2006; Stapleton et al., 2007; Piette et al., 2012; Samuelsen et al., 2012). Previous studies relying on intraoral deliveries of tastants in water-restricted rats have shown that 0.1 M S and 0.1 M N consistently evoke orofacial reactions that signal positive palatability, whereas 0.2 M C and 0.001 M Q are effective in evoking reactions that signal aversion (Fontanini and Katz, 2006; Samuelsen et al., 2013). Each trial consisted of a variable intertrial interval (30 ± 10 s), followed by a delivery of 40 μl (computer-controlled opening time ~60 ms) of one of the four tastes presented pseudorandomly. Every taste delivery was followed by ~50 μl of water rinse delivered via the second IOC. Each taste presentation was repeated for at least 10 times in each recording session.

Electrophysiological recordings. Extracellular spiking activity of single neurons was recorded using 25 μm Formvar-coated nichrome microwires. Neuronal activity was amplified, bandpass filtered (300 Hz to 8 kHz), and digitally recorded (Plexon). Single-unit action potentials were discriminated and isolated using a template algorithm, cluster cutting techniques, and examination of interspike interval plots (Offline Sorter; Plexon).

Analysis of electrophysiological data. Spike sorting and data analysis were performed by means of Offline Sorter (Plexon), NeuroExplorer (Nex Technologies), and MATLAB scripts (MathWorks). Single-neuron and population peristimulus time histograms (PSTHs) were plotted around the taste deliveries. A bin size of 200 ms was used unless otherwise specified. Neurons with peak firing rate lower than 1 Hz were excluded from further analysis to avoid statistical artifacts. Neurons with a large peak around the 6–10 Hz in the spike power spectrum were considered somatosensory (Katz et al., 2001; Samuelsen et al., 2012; Horst and Laubach, 2013) and excluded from additional analysis to avoid confounds related to mouth movements.

Taste responsiveness. Taste responsiveness was assessed by studying the single-unit cumulative distribution function (cdf) of spike occurrences across all trials for a given taste. For each neuron and for each taste, we considered the cdf in the interval starting 1 s before and ending 5 s after taste delivery. The response of a neuron to a stimulus was signaled by the occurrence of a "change point" (CP), i.e., a sudden change in firing rate during the post-stimulus interval due to a piecewise change in the slope of the cdf. To avoid detection of CPs in the baseline period, we introduced an adaptive CP procedure. Briefly, we ran the first CP sweep of the cdf at a fixed tolerance level [using the algorithm in the study by Gallistel et al. (2004), with $p = 0.05$]. If a CP was detected before taste delivery, the CP analysis was repeated from the start by decreasing the tolerance level [i.e., by increasing the logit in steps of 0.2, where logit $= \log(1 - p)/p)$], so as to make the CP detection more conservative. If no CP was detected for any of the four tastes, the neuron was deemed not responsive. If a CP was detected in the post-delivery interval for at least one taste, a *t* test was performed to establish whether taste-evoked activity was significantly different from baseline activity (1 s interval before taste delivery; $p < 0.05$). By definition, a neuron was taste responsive (TR) if at least one significant CP was found after delivery. This adaptive CP procedure was preferred to the more common practice of comparing a sequence of post-stimulus time bins to the baseline because it does not rely on binning, allowing a more precise temporal determination of the latency of responsiveness.

The time of the earliest post-delivery CP (across all tastes) was used to define the latency of the response. We characterized latencies through their medians and 68% bootstrapped confidence intervals (CIs) (Efron, 1986) due to the non-normal nature of the latency distribution (Fig. 1*C*). For the same reason, within-area latencies for different subpopulations were compared via a Kruskal–Wallis non-parametric one-way ANOVA test. Value and time of the peak response was computed by identifying the largest extremum in the smoothed PSTH (BARS algorithm of DiMatteo et al. (2001)) occurring after the first significant CP. The normalized firing rate shown in Figure 1*B* was obtained as the average across tastes and neurons of the difference between the maximal firing rate at peak minus the average firing during baseline (0.5 s before stimulus delivery). The temporal resolution to locate the peak was 50 ms.

Taste selectivity. A neuron was considered as taste-selective (TS) if its response to the stimuli varied significantly across different tastants in either magnitude or time course. Taste selectivity (Fig. 2*A*) was assessed by two different and independent methods. The first approach was based on a two-way ANOVA (taste identity × time course), using 200 ms bins in the [0, 5] s post-delivery interval. A neuron was defined TS if either the taste main effect or the interaction term was found significant (at $p < 0.01$). To determine the time course of selectivity, the taste-evoked period was divided into 200 ms bins, and the number of taste-selective neurons was computed within each bin (one-way ANOVA for taste identity, $p < 0.05$). To assess whether the time course of taste selectivity differed between the two areas, a Kolmogorov–Smirnov test was performed on the across-bins cdf of taste-selective neurons. A second approach to determine taste selectivity relied on a more sensitive classification procedure based on a decoding analysis (for details, see below, Single-neuron decoding). A neuron was defined as TS by decoding if its performance in a taste classification algorithm was significantly above chance level for at least one taste. Comparison of tuning of taste-selective neurons (Fig. 2*B*) was performed with a χ^2 test, followed, if significant, by the Marasquilo's *post hoc* test for multiple comparisons (for a detailed description of the procedure, see La Camera and Richmond, 2008).

Taste classification. To assess the amount of taste-related information in single-neuron taste profiles, we used a decoding procedure for taste classification. We considered all trials in each session and split them into four "training sets," one for each taste, and one "test set," containing all remaining trials from all tastes. We trained a classifier on the four training sets and then classified each of the test trials as belonging to one of the four conditions (S, N, C, and Q). We used a onefold or twofold cross-validation procedure. All decoding analyses were based on a maximum likelihood classifier that relies on the firing rate temporal profiles of the four tastes, using 200 ms bins in the post-delivery interval (for details, see below, Single-neuron decoding). Decoding performance was defined as

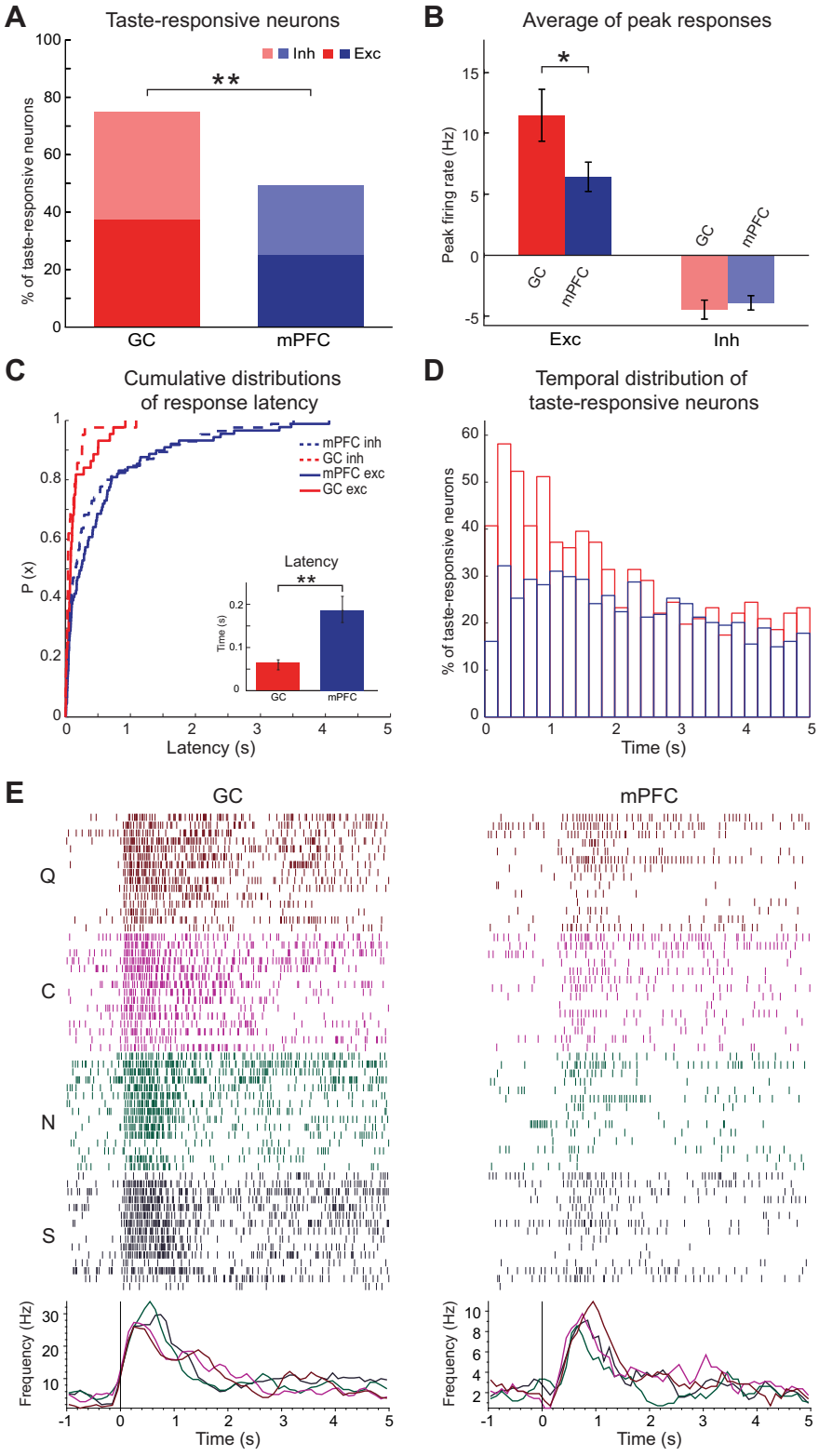

Figure 1. Responsiveness to gustatory stimulation in GC and mPFC. ***A***, Percentage of neurons whose firing rates significantly changed in the 5 s after tastants delivery. Red bar, GC; blue bar, mPFC. $^{**}p < 0.01$, χ^2 test. Excitation (dark colors; Exc) and inhibition (light colors; Inh) of the firing rate were evoked in similar proportion of neurons. ***B***, Differences in the peak firing response between GC (red bars) and mPFC (blue bars). Left bars, Excitatory responses; right bars, inhibitory responses. $^{*}p < 0.05$, *t* test. Firing rate was relative to baseline activity 0.5 s before taste delivery and averaged across neurons and tastes; for details, see Materials and Methods. Error bars indicate SEM. ***C***, Cumulative distribution of the latencies of taste responses in GC (red lines) and mPFC (blue lines). The cumulative distribution was computed for the excitatory responses (solid lines) and for the inhibitory responses (dashed lines). The inset shows the median onset of taste responses in GC (red bar) and mPFC (blue bar); error bars are 68% bootstrapped CIs. $^{**}p < 0.001$, Mann–Whitney test. ***D***, Time course of the percentage of taste-responsive neurons computed in successive 200 ms bins for the 5 s period after tastants delivery. Responses in GC (red bars) peaked at ~0.4 s, whereas in mPFC (blue bars), the responses were more homogeneously distributed over 5 s. ***E***, Raster plots and PSTH of representative taste-responsive neurons. Left, GC taste-responsive neuron. Right, mPFC taste-responsive neuron. Both neurons responded with increases in firing rates to each of the four tastants (S in dark blue; N in dark cyan; C in dark magenta; Q in dark red). Taste delivery occurs at time 0 (vertical lines).

the fraction of test trials that were classified correctly over a series of cross-validation trials (Stone, 1974; Shao, 1993). For each taste, either one or two trials were removed from the training set and then used as test trials to assess decoding performance; the procedure was repeated leaving out a single trial until all n trials had been used and leaving out a single pair until all $n(n-1)/2$ pairs of trials had been used to increase the number of test trials (Minamimoto et al., 2009). The CI (p_-, p_+) on the decoding performance p of a single unit was defined by $p_\pm = (1/2)[pn + 1/2 \pm \sqrt{[p(1-p)n + 1/4)}]/(n+1)$, where n was the total number of validation trials (La Camera et al., 2006). CIs were otherwise obtained by a bootstrap procedure in the case of population decoding or by evaluating the relevant percentiles of the performance distribution when pooling across single neurons (for details, see below).

Single-neuron decoding. In single-neuron trial-by-trial decoding, each tastant was represented by a point in an M-dimensional vector space of firing rates, where M was the total number of temporal bins after delivery and each entry was the average firing rate across all trials in the training set in a particular bin; each trial from the test set was then classified according to the smallest Euclidean distance from the four training points in such M-dimensional space. Under some standard assumptions, this procedure can be understood as approximating a maximum likelihood classifier (Press et al., 2007). Misclassifications led to false positives for which we adopted the following nomenclature (see Results, Coding of taste hedonic value, and Fig. 4): an S test trial erroneously classified as Q is referred to as a Q false positive in S trials, and similarly for all other cases.

Population decoding. To perform a population decoding analysis of taste, we constructed a "pseudopopulation" of neurons, collecting units from different sessions and animals under the same stimulus condition. Each tastant was represented as a point in an $N \times M$-dimensional vector space of firing rates, where N is the number of units included in the pseudopopulation (units from sessions with at least 10 trials for each taste were considered), and M is the number of temporal bins. Statistical significance of decoding was assessed with a bootstrap procedure, by sampling with replacement a subset of 80% of the neurons from the whole population for each bootstrap run (50 bootstrap runs were used). In each run, decoding performance was assessed via the Euclidean distance as done for the single-neuron

←

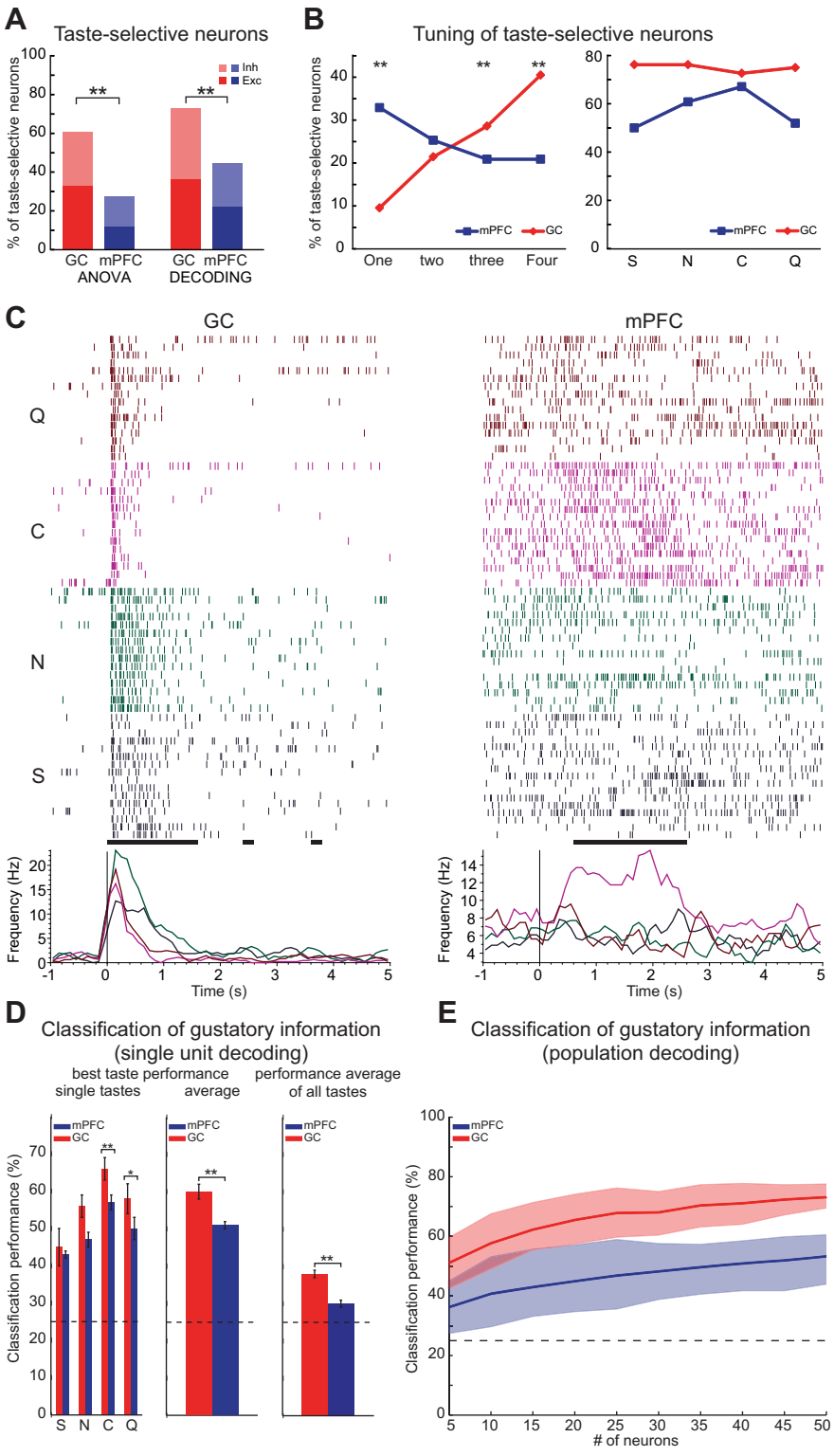

Figure 2. Taste-selective responses in mPFC and GC. ***A***, Percentage of neurons that responded selectively to one or more tastant. Taste selectivity was assessed using two different methods: a two-way ANOVA test (left bars) and a decoding algorithm (right bars). $^{**}p < 0.01$, χ^2 test. ***B***, Tuning of taste-selective neurons (according to the decoding algorithm of ***A***). Left, Percentage of neurons that respond selectively to one, two, three, or four tastes in GC (red) and mPFC (blue). Right, Percentage of taste-selective neurons that responded to S, N, C, and Q, respectively. $^{**}p < 0.01$, *post hoc* Marascuilo's test (see Materials and Methods). ***C***, Raster plots and PSTH of representative taste-selective neurons. Left, A GC neuron that is selective to four tastants. Right, An mPFC neuron that is selective to one tastant. The black dots under the rasters mark bins of significant taste-selectivity (*t* test, $p < 0.05$). ***D***, Classification of gustatory information based on the activity of single taste-selective neurons. Left, Histogram indicating the percentage of trials that were correctly attributed (hits) to the tastant delivered (best taste per unit only): S, N, C, and Q. Middle, Histogram showing the average best performance across taste-selective neurons (see Results). Right, Histogram showing the average overall performance across taste-selective neurons and across all the tastants. Red, GC; blue, mPFC. $^{*}p < 0.05$, $^{**}p < 0.01$, χ^2 test. Error bars indicate SEM. ***E***, Population-based classification of gustatory information as a function of population size. Solid lines (red: GC; blue: mPFC) indicate the percentage correct decoding across all tastants. The *x*-axis indicates the number of neurons used for classification. Significant difference between GC and mPFC was fixed at $p < 0.05$ and false discovery rate corrected for multiple comparisons (shaded areas). For details, see Materials and Methods.

case (see above) but this time summing over both bins and neurons of the subpopulation. To study the relationship between decoding accuracy and the size of the pseudopopulation (Fig. 2*E*), we constructed a sequence of increasingly larger pseudopopulations, starting from a pool of five units, in incremental steps of five units. For each fixed size of the subpopulation, we computed the decoding accuracy for taste classification in each of 50 bootstrap runs, each time drawing with replacement a different random subset of units from the appropriate subpopulation. In all cases, we matched the number of neurons in each subpopulation in GC with the number in each subpopulation in mPFC. Bootstrap CIs were used to compare performance of GC versus mPFC ensembles. Multiple comparisons were corrected by controlling the false-discovery rate (Benjamini and Hochberg, 1995). To estimate the minimal number of neurons needed to reach a decoding accuracy of 95%, we created a large surrogate neuronal population from the available data (Rigotti et al., 2013). For each area, we considered the population of taste-selective units (based on the decoding procedure) and resampled the recorded neurons by randomly reassigning the labels of the spike responses to different tastes. For example, the recorded activity of a particular neuron in response to, respectively, S, N, C, and Q, was reassigned to the response of a new surrogate neuron to, respectively, Q, C, N, and S. This procedure was repeated for all $4! = 24$ possible permutations of the four taste labels, giving a neural population 24 times larger than the recorded one (for a more detailed description of the procedure, see Rigotti et al., 2013). We then proceeded with the same bootstrapped population decoding procedure as described above.

The analysis of the time course of decoding (Fig. 3*C*) was performed using a decoding window of 200 ms, stepping along at 50 ms steps, with a bootstrap procedure applied in each window, as described above.

We performed a comparative analysis of latencies of taste coding onsets in the two areas in which latency of coding is defined as the first bin, in which the taste decoding performance is significantly above chance level. To control for the difference in firing rates between the two areas, we first transformed each unit response into *z*-scores, defined as $z = (x - \mu)/\sigma$, where x is the single-trial firing rate in each post-delivery bin, μ is the average baseline firing rate, and σ its stan-

←

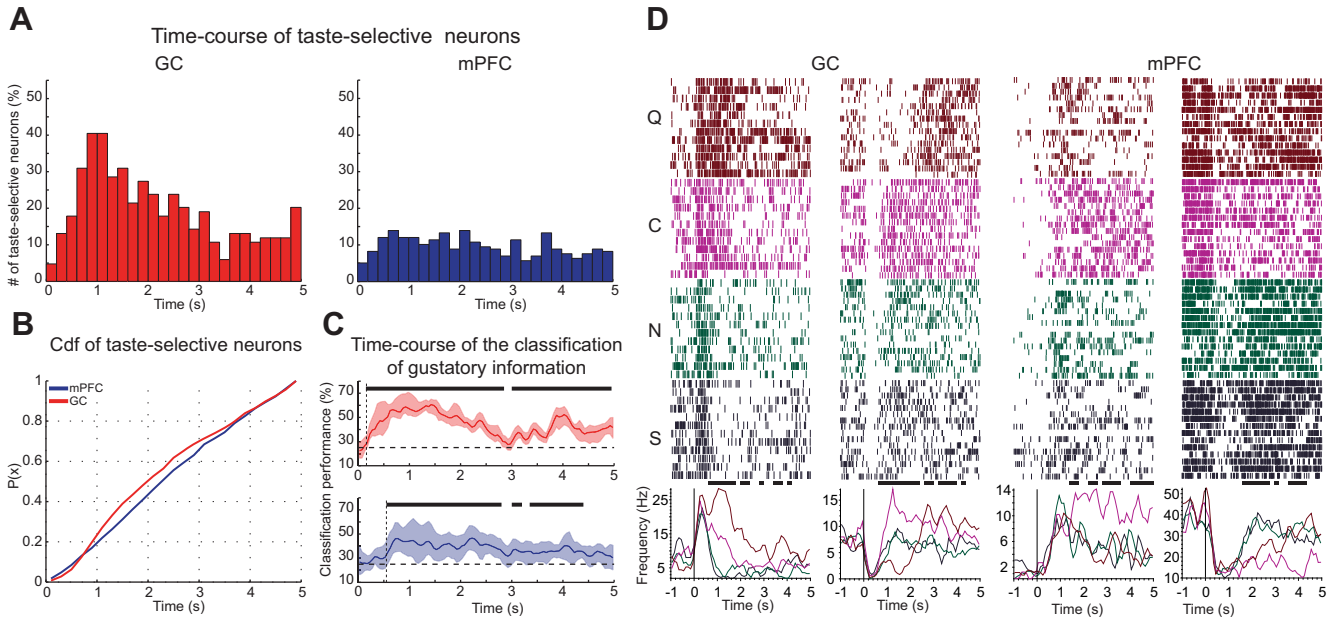

Figure 3. Time course of chemosensory processing in mPFC and GC. ***A***, Time course of taste selectivity computed in successive 200 ms time-bin size over 5 s after the tastants delivery. Each bar represents the percentage of neurons that are TS in a given time bin. The distribution of taste-selective neurons peaks in the two bins at ~1 s in GC, and it is more homogenously distributed in mPFC. ***B***, Cumulative distribution of the percentage of taste-selective neurons as a function of time. ***C***, Time course of the classification of gustatory information. Solid lines (red, GC; blue, mPFC) represent the percentage of correctly classified trials based on the population activity. Shading around traces: 95% bootstrapped CI; solid lines above trace represent significance from chance levels (95% bootstrapped CI above chance level) for a consecutive interval larger than the moving window bin size (200 ms). Vertical dashed lines indicate the decoding latency. ***D***, Raster plots and PSTHs of representative selective neurons showing the time course of taste selectivity in GC (left) and mPFC (right). Black lines represent times at which responses are TS as determined with a one-way ANOVA ($p < 0.05$).

dard deviation; then, we normalized each unit z-score to its absolute value peak across all trials and events. Finally, we performed the population decoding as outlined above, replacing the firing rates with normalized z-scores.

Palatability analyses. We used several independent analyses to assess the palatability-related information content of neuronal responses to taste delivery. To assess whether the response of a neuron encoded palatability-related information that was not related to its taste specificity, we used the taste-classification procedure described above but focused on the misclassification rate rather than the decoding performance. By definition, a neuron encoded palatability-related information (but not correct taste identity) if it misclassified rewarding S and N test trials as either N or S but not as aversive C or Q (or vice versa for information related to aversive tastes). More precisely, we defined a responsive neuron as palatability specific (PS) if (1) the misclassification of test trials was significantly above chance (χ^2 test, $p < 0.01$) and (2) the misclassification into tastes with the same palatability as the test trials was larger than the misclassification into tastes of the opposite palatability. As a second measure of how single-unit responses reflect palatability, we considered the time course of the difference in the PSTHs in response to tastes of the same versus opposite palatability (Piette et al., 2012) to build a measure of palatability-related information that we call the palatability index (PI; defined below). Neurons in GC showed a larger firing rate response to taste delivery with respect to neurons in mPFC, which might introduce a bias in the estimate of the PI. To remove this bias, we first normalized the PSTHs in both areas according to the receiver operating characteristic (ROC)-based procedure (Cohen et al., 2012). Briefly, we compared the histogram of spike counts during the baseline period with that during a given bin by moving a criterion from zero to the maximum firing rate. We then plotted the probability that the activity during the chosen bin was greater than the criteria against the probability that the baseline activity was greater than the criteria. For each bin, the area under this curve is the ROC-normalized PSTH for that bin; this is a number between zero and one and quantifies the degree of overlap between the two spike count distributions (i.e., the discriminability of the two). Values larger than 0.5 express the likelihood that the firing rate in the bin is above baseline, whereas values below 0.5 express the likelihood that the firing rate in the bin is below baseline (for details, see Cohen et al., 2012). The PI was then computed as follows. We first evaluated the average of the absolute value of the log-likelihood ratio of taste responses with the same and opposite palatability:

$$\langle|\mathrm{LR}|\rangle_{\mathrm{same}} = \frac{1}{2}\left(\left|\ln\frac{S}{N}\right| + \left|\ln\frac{Q}{C}\right|\right), \langle|\mathrm{LR}|\rangle_{\mathrm{opposite}} = \frac{1}{4}\left(\left|\ln\frac{S}{C}\right| + \left|\ln\frac{S}{Q}\right| + \left|\ln\frac{N}{C}\right| + \left|\ln\frac{N}{Q}\right|\right),$$

where S, N, C, and Q denote the value of the ROC-normalized PSTH in S, N, C, and Q trials, respectively. We then defined the PI as the difference between those two averages, i.e., $\mathrm{PI} = \langle|\mathrm{LR}|\rangle_{\mathrm{opposite}} - \langle|\mathrm{LR}|\rangle_{\mathrm{same}}$. A positive PI value suggests that a neuron responds similarly to tastes with the same palatability and differently to tastes with opposite palatability. A negative PI value indicates the opposite.

Spatial distribution of recorded neurons. Possible spatial clustering of response types (i.e., taste-selective vs palatability-specific) was assessed by comparing the depth distributions of taste-selective, palatability-specific, and taste-unresponsive neurons using a Kolmogorov–Smirnov test.

Histological procedures. At the end of the recording experiments, rats were anesthetized (ketamine–xylazine–acepromazine mixture at 100, 5.2, and 1 mg/kg, respectively), and electrolytic lesions (7 μA cathodal current for 7 s) were made through selected wires to mark electrode positions. Subsequently, subjects were perfused through the left cardiac ventricle with saline, followed by 10% Formalin. All solutions were prepared in phosphate buffer (0.1 M, pH 7.4). Fixed brains were stored in 10% Formalin and cut into 60-μm-thick coronal sections. The sections were stained using standard Nissl procedures, and the correct positioning of electrodes was verified by assessing the electrode tracks. Location of the neurons recorded was estimated *post hoc* on the basis of histological reconstruction, measurement of initial positioning during the surgery, and measurement of electrode advancement. In mPFC, neurons re-

corded at depths 2.5–3.3 and 3.3–4.1 mm from the surface were classified as belonging to prelimbic and infralimbic areas, respectively. As for GC, neurons were recorded between 4.3 and 5.9 mm from the surface of the brain.

Results

Responsiveness to gustatory stimulation

The data presented here come from the analysis of 354 and 115 neurons, recorded in mPFC and GC, respectively, from eight freely moving rats passively receiving tasting solutions through IOCs.

To begin evaluating the differences in taste responsiveness between the two areas, the number of neurons significantly changing their firing rates in the first 5 s after gustatory stimulation was compared. As Figure 1*A* shows, firing activity in mPFC neurons is significantly modulated by taste delivery. Of the 354 mPFC neurons recorded, 174 (49%) significantly changed their firing rates in response to gustatory stimulation; excitatory and inhibitory responses (i.e., increases and decreases in firing rates) were observed in a similar proportion of neurons [51% (89 of 174) of excitatory responses against 49% (85 of 174) of inhibitory responses]. The proportion of taste-responsive neurons was significantly lower in mPFC than in GC [49% (174 of 354) vs 75% (86 of 115) of taste-responsive neurons in mPFC and GC respectively, $\chi^2_{(1)} = 24$, $p < 0.001$], but the relative proportion of excitatory and inhibitory responses was similar in the two areas [GC: 50% (43 of 86) of each type of response; mPFC: 51% excitatory (89 of 174), 49% inhibitory (85 of 174); Fig. 1*A*]. To assess the magnitude of responses to taste, peak firing rates in response to gustatory stimulation were computed for neurons with excitatory and inhibitory responses (Fig. 1*B*, firing rates are normalized to baseline). Peak inhibitory responses were similar in mPFC (-3.9 ± 0.6 Hz, $n = 85$) and GC (-4.4 ± 0.8 Hz, $n = 43$), but peak excitatory responses were significantly higher in GC compared with mPFC (11.4 ± 2.1 Hz, $n = 43$ for GC vs 6.4 ± 1.2 Hz, $n = 89$ for mPFC; *t* test, $t_{(69)} = 2.1$, $p < 0.05$). Next, the temporal structure of taste responses in the two areas was compared. Figure 1*C* shows the cdf of the response latency computed relying on a change point (CP) analysis (for details, see Materials and Methods). The median onset of responses across the two areas was significantly different (Mann–Whitney $U = 4423$, $r = 0.4$, $p < 0.001$): it was 0.19 s (CI = 0.16, 0.22 s; $n = 174$) in mPFC and 0.06 s (CI = 0.05, 0.07 s; $n = 86$) in GC (Fig. 1*C*, inset). A larger proportion of neurons responded in the first 250 ms in GC than in mPFC, as confirmed by the cumulative distribution plot in the main panel of Figure 1*C*. Hence, changes in taste-evoked firing activity occurred earlier in GC than mPFC. The overall temporal distribution of responses also revealed differences between the two areas. As shown in Figure 1*D*, which displays the distribution in time of significant changes in firing rates evoked by tastants, responses in GC peaked at ~0.4 s after taste delivery. Firing rate modulations in mPFC appeared to be more homogeneously distributed over the 5 s windows examined. Figure 1*E* features representative raster plots and PSTHs for GC (left) and mPFC (right) neurons with excitatory responses to the four tastants delivered (S, N, C, and Q). Inspection of these plots confirms the results presented above indicating that excitatory responses are stronger and faster in GC than mPFC.

Taste selectivity and coding of taste quality

It is well established that neurons in GC do not simply respond to gustatory stimulation with a specific modulations of their firing rates, they fire differently to different tastants (Katz et al., 2001; Samuelsen et al., 2012, 2013; Maier and Katz, 2013). To evaluate the ability of mPFC to process gustatory information, the number of neurons responding selectively to one or more taste qualities was computed (for definition of taste selectivity, see Materials and Methods). Figure 2*A* displays the comparison for the number of taste-selective neurons in mPFC and GC. Neurons in mPFC can selectively respond to specific taste qualities, but the proportion of taste-selective neurons is smaller in mPFC than GC as shown in Figure 2*A*. When using a conservative measure of selectivity, i.e., positivity to a two-way ANOVA test (see Materials and Methods), 28% (98 of 354) of the mPFC neurons appeared to respond selectively to different stimuli (vs 61%, 70 of 115, in GC, $\chi^2_{(1)} = 41$, $p < 0.001$). Use of a more sensitive decoding algorithm revealed a higher proportion of taste-selective cells in mPFC (45%, 158 of 354), yet the number was still lower than that observed with the same method for GC (73%, 84 of 115; $\chi^2_{(1)} = 27$, $p < 0.001$). To assess differences in breadth of tuning, the proportion of neurons that responded specifically to one, two, three, or four tastants was computed (Fig. 2*B*, left). This analysis revealed significant differences between mPFC and GC distributions ($\chi^2_{(7)} = 94$, $p < 0.01$). A *post hoc* analysis revealed that, although the proportion of neurons that responded to one tastant only was higher in mPFC than GC (mPFC, 33%, 52 of 158; GC, 10%, 8 of 84; Marasquilo's test, $p < 0.01$), the opposite was true for neurons that showed taste-selective responses to all four stimuli (mPFC, 21%, 33 of 158; GC, 40%, 34 of 84; Marasquilo's test, $p < 0.01$). To determine differences in how each taste was represented in mPFC, the distribution of neurons encoding for each of the four tastes was determined. Figure 2*B*, right, shows that, although the four tastes were encoded homogeneously in GC ($\chi^2_{(3)} = 0.4$, $p > 0.9$), mPFC showed a modulation in the preference for taste quality ($\chi^2_{(3)} = 12$, $p < 0.01$). Figure 2*C* shows raster plots for two representative units: a broadly tuned GC neuron (left) and an mPFC neuron responding to a single tastant (right).

To assess the impact of differences between the two areas on taste coding, GC and mPFC performances in correctly classifying gustatory information were computed. Single-neuron ability in encoding taste quality was quantified by computing the best classification performance for each taste quality and for each taste-selective neuron in mPFC and GC. This analysis amounted to decoding single-trial firing rates over 5 s after the presentation of the stimulus (see Materials and Methods). Figure 2*D* shows the across-neuron average performance for each of the four stimuli for mPFC and GC. The left in Figure 2*D* shows the across-neuron average best classification for each tastant. For both mPFC and GC, the classification was above chance level for all tastants (GC, $\chi^2_{(7)} = 22$; mPFC, $\chi^2_{(7)} = 25$; $p < 0.01$) and was significantly different between the two areas (two-way ANOVA, main effect, $F_{(1,56)} = 9.2$, $p < 0.01$). The middle shows that the overall best performance across neurons was lower in mPFC than in GC (mPFC, $51 \pm 1\%$, $n = 158$ neurons; GC, $60 \pm 2\%$, $n = 84$ neurons; *t* test, $t_{(240)} = 4.0$, $p < 0.001$; for each neuron, its "preferred taste" was used, i.e., the taste having best classification performance). We also computed the average across all taste-selective neurons and across all four tastes, as shown in the right of Figure 2*D*. Also in this case, the performance for mPFC was significantly lower than for GC (mPFC, $30 \pm 1\%$, $n = 158$ neurons; GC, $38 \pm 1\%$, $n = 84$ neurons; *t* test, $t_{(618)} = 5.6$, $p < 0.001$).

Taste coding in the two areas was further evaluated using a decoding analysis performed on the basis of ensemble data. Figure 2*E* shows the decoding performance for mPFC and GC ensembles as the number of neurons used for the classification increased. As expected, maximal performance was greatly in-

creased by pooling multiple neurons. Ensemble decoding of tastants was significantly different between the two areas (two-way ANOVA, area effect, $F_{(1,1470)} = 2641$ and population size effect, $F_{(14,1470)} = 85$, both $p < 0.001$). Although for ensembles of five neurons the performance between the two areas was similar ($\chi^2_{(1)} = 2.5$, $p > 0.1$), GC performance was notably higher than that for mPFCs for classifications based on groups of neurons larger than 20 units ($\chi^2_{(1)} = 4.4$, $p < 0.05$). The maximal performance occurred for the largest population of neurons ($n = 50$), giving a correct classification performance of 73 ± 4% for GC and 53 ± 7% mPFC ($\chi^2_{(1)} = 5.5$, $p < 0.05$). Both values are significantly higher than average performance of single neurons (GC, 38%, $\chi^2_{(1)} = 15.4$, $p < 0.001$; mPFC, 30%, $\chi^2_{(1)} = 8.7$, $p < 0.01$).

To quantify the size of the population needed to decode tastants in a highly accurate manner (>95% correct), we created surrogate neuronal ensembles (using the procedures described by Rigotti et al., 2013; see Materials and Methods). A bootstrapped population decoding procedure was used on pseudo-ensembles of increasing numbers of neurons. The minimal number of neurons needed to reach 95% performance was 190 for GC and 300 for mPFC. This analysis further confirms that GC encodes taste more efficiently than mPFC, yet the absolute number of neurons needed for encoding taste in a highly accurate manner is relatively low for both areas.

Altogether, these data show that information pertaining to the chemosensory identity of gustatory stimuli is represented in mPFC single-neuron and ensemble activity. However, relative to GC, mPFC showed a significantly lower number of taste-selective neurons and a lower ability to encode taste identity.

Time course of chemosensory processing

Taste evokes time-varying chemosensory responses in multiple brain regions (Katz, 2005; Di Lorenzo et al., 2009; Gutierrez et al., 2010). To investigate the differences between mPFC and GC, the temporal structure of chemosensory responses in the two areas was compared. Figure 3*A* shows the results of a quantification of the temporal distribution of chemosensory neurons in mPFC and GC. Each bar in the plot indicates the number of neurons that are TS within each time bin. In accordance with previous work (Piette et al., 2012; Samuelsen et al., 2012), the number of taste-selective GC neurons peaks between ~0.5 and ~1.5 s. Conversely, in mPFC, the temporal distribution of taste responsiveness appears to be flat and sparse. This difference can be observed in Figure 3*B*, featuring the significantly different cumulative distributions of taste selectivity in time (Kolmogorov–Smirnov test, $k_{(274)} = 0.38$, $p < 0.001$).

Additional analyses were performed to determine the latency of chemosensory coding in GC and mPFC. In the two areas, the time course of a classification analysis was computed for the populations of taste-selective neurons in mPFC and GC (for this analysis, a population of 67 neurons was used in both areas, which amounts to 80% of the taste-selective neurons in GC for each bootstrap run; see Materials and Methods). Figure 3*C* shows the bin-by-bin classification performance based on population activity over 5 s after taste delivery for GC (top) and mPFC (bottom). Although populations in both areas show a significantly above chance classification performance (black solid line above traces, 95% bootstrapped CI above chance level), the onset of coding differed for the two areas, with GC neurons allowing for shorter-latency classification than mPFC neurons. The earliest time at which GC ensembles encoded taste significantly above chance was 175 versus 575 ms for mPFC. At 175 ms, coding in GC was significantly higher than in mPFC (*t* test, $t_{(49)} = 7.2$, $p < 0.001$). Additional analyses were performed on normalized responses to determine whether the difference in latency depended on differences in firing rates between GC and mPFC. Single-neuron responses were normalized using a two-step procedure: first the *z*-score was computed, and then the score of each neuron was normalized to its maximum *z*-score. The second step of this procedure was implemented specifically to eliminate differences in maximal firing rates between neurons and thus eliminate the potential confound of weak responses on the assessment of latency. The same classification procedures described above were applied to the normalized dataset. Quantification of the latency of taste coding confirmed that GC encodes identity more rapidly than mPFC (GC, 75 ms; mPFC, 225 ms), indicating that the difference in onset is related to the tuning of responses rather than the magnitude.

Figure 3*D* features raster plots and PSTHs from representative neurons showing area-dependent latency of chemosensory coding. Both the excitatory and inhibitory responses in mPFC become TS after ~1.5 s after tastant delivery. Conversely, GC neurons show selectivity well before ~1 s.

Coding of taste hedonic value

Taste quality is not the only feature encoded by cortical neurons; in fact, taste palatability is also processed in GC (Accolla and Carleton, 2008; Grossman et al., 2008; Sadacca et al., 2012). On the basis of the literature, it is reasonable to expect that rat mPFC might encode palatability at least as well as GC (Amiez et al., 2006; Petykó et al., 2009; Horst and Laubach, 2013). To address this issue, the number of neurons whose firing rate activity encoded palatability information was computed. A neuron was considered to encode palatability if it responded similarly to stimuli that belonged to the same hedonic category (i.e., rewarding, S and N; or aversive, Q and C) and differently to stimuli that had opposite hedonic value (Fontanini et al., 2009; Piette et al., 2012). Similarity and differences of responsiveness were assessed using a decoding algorithm (see Materials and Methods). Figure 4*A* shows the results of this quantification. No significant difference was observed in the proportion of taste-responsive neurons that encoded palatability in mPFC and GC (mPFC, 26% of the taste-responsive neurons, 46 of 174; vs GC, 21% of the taste-responsive neurons, 18 of 86, $\chi^2_{(1)} = 0.9$, $p > 0.3$). This result was confirmed when neurons were grouped depending on whether they produced excitatory or inhibitory responses to taste. Neither of the groups showed a significant difference in the two areas. A classification analysis was performed on palatability encoding neurons to determine differences in their overall performance. This analysis computed the across-neuron average classification performance for each tastant. The results shown in Figure 4, *B* and *C*, confirm that, in both areas, these neurons encode for palatability. Palatability-encoding neurons in GC displayed the best performance for the actual stimulus delivered, but in all instances, the highest scoring false positive was a tastant belonging to the same hedonic category as the one presented. For instance, as Figure 4*B*, left, shows GC neurons correctly classify S deliveries, and when they fail to do so, the most common confusion is between S and N (i.e., S, 35%, N false positive: 29%; N, 39%, S false positive: 28%; C, 56%, Q false positive: 22%; Q, 39%, C false positive: 34%). Differently from GC neurons, mPFC palatability neurons encoded preferentially palatability over identity. In fact, tastants were classified more accurately according to palatability than identity. Except for the citric acid, the decoding performance in

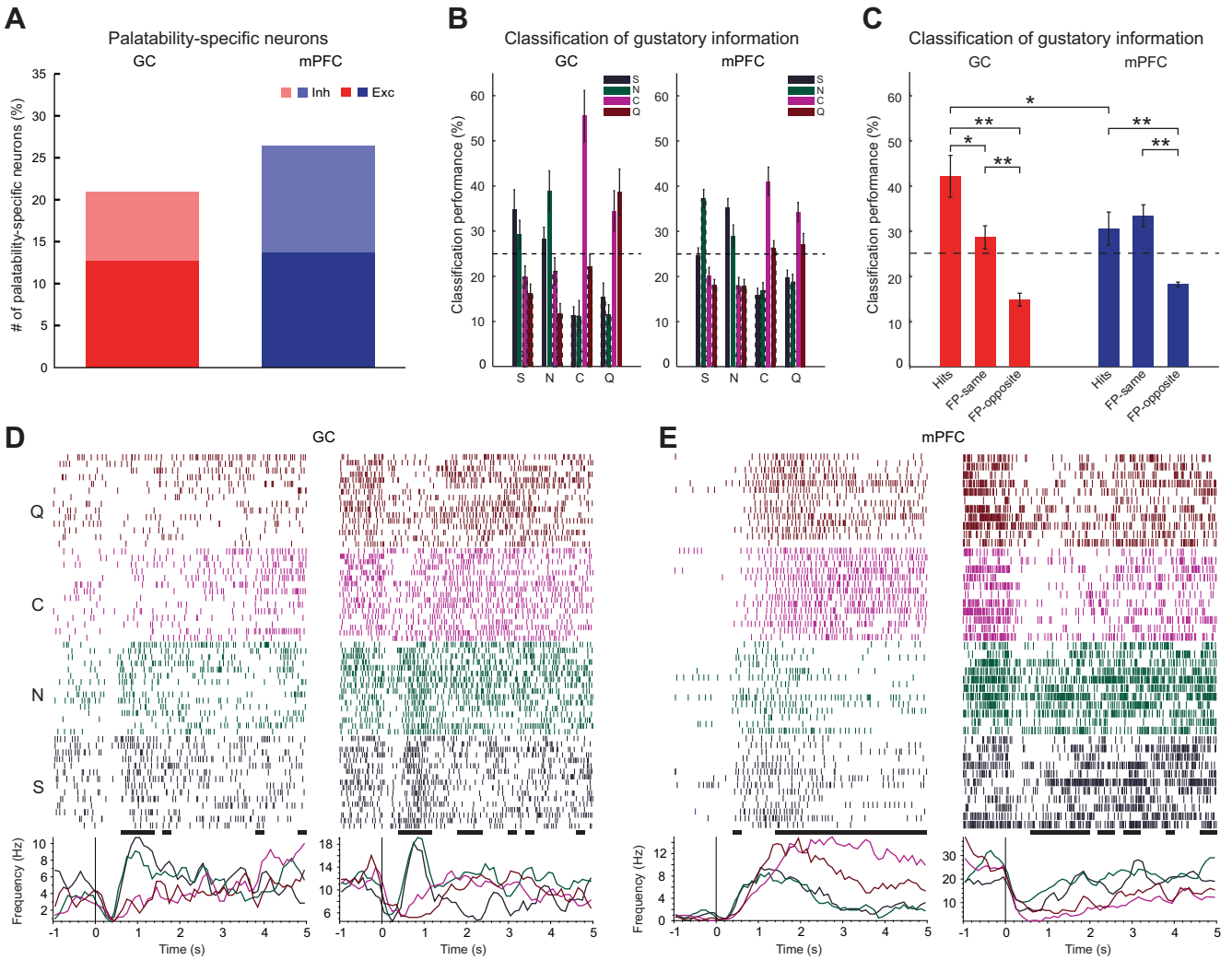

Figure 4. Coding of palatability in mPFC and GC. ***A***, Percentage of neurons whose firing rates showed specificity to taste palatability (i.e., similar firing pattern between tastants with the same palatability and different firing pattern between tastants with the opposite palatability). Left, GC; right, mPFC. ***B***, Histograms showing taste classification performance for palatability-specific neurons in GC (left) and mPFC (right). Each group of bars indicates the percentage of trials classified for each of the tastants. The label under the plot indicates the actual delivered tastant, and the color of each bar indicates the tastant determined by the classifier. Dashed lines around bars indicate the significant difference ($p < 0.05$) from the delivered taste. Error bars indicate SEM. ***C***, Average classification in GC (red) and mPFC (blue) for correct hits (hits), false-positive errors for tastants with same palatability (FP-same), and false positive errors for tastants with opposite palatability (FP-opposite); *$p < 0.05$; **$p < 0.01$, *t* test. ***D***, Raster plot and PSTHs of representative palatability-specific neurons. Left, Two GC palatability-specific neurons (left). Right, Two mPFC palatability-specific neurons. Error bars indicate SEM.

mPFC was at least as good for the nonstimulus tastant with the same palatability as the stimulus than for the delivered stimulus itself, suggesting a high degree of similarity between responses to stimuli with similar hedonic value (i.e., S, 25%, N false positive: 37%; N, 29%, S false positive: 36%; C, 41%, Q false positive: 26%; Q, 27%, C false positive: 34%;). Figure 4*C* features the results of averaging correct classifications (Hits), similar-palatability false positives (FP-same), and false positives for tastants of opposite palatability (FP-opposite) across neurons in GC (red bars) and mPFC (blue bars). The results indicate that, whereas in GC correct classification was more likely than misclassification (42 ± 5 vs 28 ± 3%, *t* test, $t_{(14)} = 4.8$, $p < 0.01$), in mPFC, the probability of these two events was not significantly different (30 ± 4 vs 33 ± 2%, *t* test, $t_{(14)} = 1.6$, $p > 0.1$). Figure 4, *D* and *E*, shows four representative neurons recorded in GC and mPFC. Visual inspection of the rasters clearly highlights the similarity between responses to similarly palatable stimuli.

Temporal dynamics of palatability-related responses

To gain insight into the temporal structure of palatability-related response, the time course of a palatability response was computed. This response was obtained by determining, for each neuron, the palatability index (PI; see Materials and Methods). The population PIs for GC and mPFC are shown in Figure 5*A*. Comparison of the two PIs clearly shows differences in the time course (left panel, GC; right panel, mPFC): GC showed a pronounced peak in the PI between 0.6 and 1.2 s, whereas mPFC showed a more tonic palatability response in the PI starting at 0.8 s and sustained until 5 s. The analysis of single-unit PIs revealed that the across-neurons average onset of the significant palatability response was similar in the two areas (mPFC, 0.63 ± 0.06 s, $n = 46$; GC, 0.67 ± 0.15 s, $n = 18$). Neural responses in mPFC carried palatability information for longer than GC (see solid black bar above traces, indicating periods of significantly above-baseline values, *t* test, $p < 0.05$), up to 5 s after stimulus delivery. To further analyze the time course of palatability-related

responses, the population PSTHs were computed for neurons encoding palatability in the two areas. Specifically, to determine whether GC or mPFC showed across-neuron patterns of responses to palatable and aversive stimuli, population PSTHs for tastants with similar palatability were averaged (Fig. 5*B*). Analysis of excitatory responses in GC revealed little differences between responses to the two categories of stimuli. Significant differences between responses to palatable and aversive tastants (black lines above traces, *t* test, $p < 0.05$) were observed in GC for a window from 1 to 2.6 s, with excitatory responses to rewarding stimuli lasting slightly longer than responses to aversive tastants (Fig. 5*B*, left top). Palatability-specific patterns confined between 0.6 and 1.2 s after stimulus delivery were observed also for inhibitory responses (Fig. 5*B*, left bottom). However, differently from excitatory responses, strong inhibitory responses lasted longer for aversive stimuli than responses to S and N (1.2 vs 0.6 s). Visual inspection of the mPFC population PSTHs featured in Figure 5*B*, right, immediately suggests a strong and long-lasting grouping of responses for tastants with similar hedonic value. Comparison of patterns in mPFC revealed a difference between activity evoked by palatable and aversive stimuli that was consistent for both excitatory and inhibitory responses. In both cases, aversive stimuli evoked significantly stronger excitatory and inhibitory responses than palatable ones. Inspection of Figure 5 clearly reveals a significant difference between responses to the two categories of stimuli; these differences emerge ~1.5 s after stimulus presentation and remain in place until the delivery of a water rinse at 5 s.

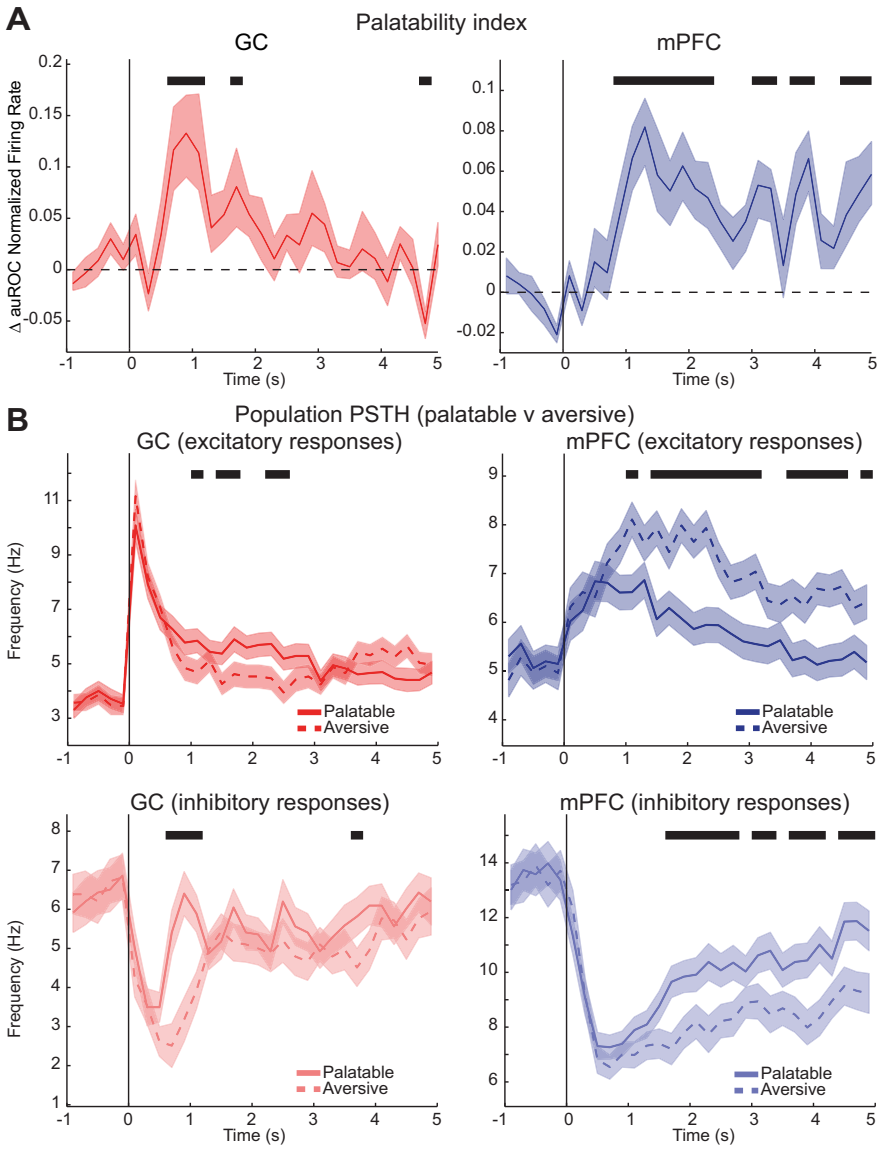

Figure 5. Time course of the palatability coding. ***A***, Time course of PI measured for 200 ms wide bins over 5 s after delivery of the tastant. Left, GC; right, mPFC. Shaded areas indicate the SEM. Black lines indicate bins in which the PI is significantly different from baseline (*t* test, $p < 0.05$). ***B***, Population PSTHs plotted for palatable (i.e., S and N, solid lines) and aversive (i.e., C and Q, dashed lines) tastants. Top row shows population PSTHs for excitatory responses and bottom row for inhibitory responses. Black lines indicate bins in which population PSTHs for palatable and aversive tastants are significantly different (*t* test, $p < 0.05$).

Comparison between GC and mPFC responses reveals significantly different profiles, with mPFC showing a bias toward aversive gustatory stimuli than GC. Additionally, divergence between responses to palatable and aversive stimuli has a later onset and a longer duration in mPFC than in GC. The onset of the significant divergence between responses to palatable and aversive stimuli was 1 s for excitatory and 1.6 s for inhibitory responses in mPFC versus 1 s for excitatory and 0.6 s for inhibitory in GC. The overall time over the 5 s window in which responses were grouped according to palatability was 3.2 s (for excitatory responses) and 2.8 s (for inhibitory responses) in mPFC versus 1 s (for excitatory responses) and 0.8 s (for inhibitory responses) in GC. Representative examples of mPFC neurons displaying responses biased toward aversive gustatory stimuli are featured in Figure 4*E*. Both the excitatory and the inhibitory examples of mPFC neurons show the characteristic late onset and long-lasting strong response to Q and C.

Within-area comparison of neural responses

Neurons in mPFC and GC can be taste-responsive (i.e., change their firing rates after taste delivery, TR), taste-selective (i.e., express a different response for different tastants, TS), and palatability-specific (i.e., express responses that correlate with the hedonic value of the taste, PS). To assess possible differences between these groups of neurons, a within-area comparison of relative proportions and dynamics was performed. In mPFC, 49% (174 of 354) of the neurons recorded were TR; of these, 56% (98 of 174) were TS, and 26% (46 of 174) were PS. In GC, 75% (86 of 115) of the neurons recorded were TR; of these, 81% (70 of 86) were TS, and 21% (18 of 86) were PS. Using the more sensitive decoding method for assessing taste selectivity greatly increased the proportion of taste-selective neurons in both GC (to 98% of responsive, 84 of 86) and mPFC (to 91% of responsive, 158 of 174). This result suggests that most taste-responsive neurons encode information regarding tastants.

Additional analyses were performed to determine the degree of overlap between taste- and palatability-specific groups. The majority (mPFC, 72%, 126 of 174; GC, 81%, 70 of 86) of the

neurons that responded to taste encoded selectively for only one specific variable. For instance, in mPFC, 68% (119 of 174) of taste-responsive neurons were TS without being PS ("TS_only"), and just 4% (7 of 174) encoded exclusively palatability ("PS_only," i.e., not TS). In GC, the proportions were similar: TS_only, 79% (68 of 86) of taste-responsive neurons; PS_only, 2% (2 of 86). In both areas, however, a group of taste-responsive neurons recorded (mPFC, 22%, 39 of 174; vs GC, 19%, 16 of 86) encoded more than one variable over time. For instance, 25% (39 of 158) and 19% (16 of 84) of taste-selective neurons in mPFC and GC, respectively, encoded both taste selectivity and palatability. This result indicates that processing of information regarding different aspects of taste consumption in both mPFC and GC is not exclusively performed by very selective neurons; on the contrary, processing of gustatory information seems widely distributed over neurons with mixed selectivity to various aspects of gustation (Rigotti et al., 2013).

Additional analyses were performed on these neurons to determine whether or not there was any within-area difference in the latency of encoding for unspecific taste responsiveness, taste identity, and taste palatability. In mPFC, TR neurons became responsive at 0.19 s (0.16, 0.22 s), TS neurons started to encode identity 0.22 s (0.17, 0.22 s), and PS neurons began to encode palatability at 0.8 s (0.5, 0.9 s). In GC, TR neurons were responsive as early as 0.06 s (0.05, 0.07 s), TS neurons began to encode identity at 0.20 s (0.12, 0.28 s), and PS neurons encoded palatability with a latency of 0.5 s (0.5, 0.7 s). Within-area subpopulation latencies were significantly different in both areas (Kruskal–Wallis one-way unbalanced ANOVA; mPFC, $\chi^2_{(2)} = 36$, $p < 0.001$; GC, $\chi^2_{(2)} = 32$, $p < 0.001$). *Post hoc* multiple comparison analyses revealed that, in mPFC, both TS and TR latencies were significantly ($p < 0.05$) different from PS ones (but not from each other), whereas in GC, all subpopulation latencies significantly differed ($p < 0.05$). These results suggest a sequential processing of different components of a gustatory experience in mPFC and GC.

To investigate whether TS and PS neurons were located in distinct divisions of the mPFC and GC, the depth profile of the distributions of the locations of the TS, PS, and taste-unresponsive neurons (see Materials and Methods) were compared using a Kolmogorov–Smirnov test. No significant clustering of response type was observed in mPFC. TS and PS neurons showed depth profiles that were not statistically different from the distribution of neurons unresponsive to taste (PS vs non-PS, $k_{(35)} = 0.12$, $p = 0.66$; TS vs non-TS, $k_{(51)} = 0.07$, $p = 0.93$). A similar analysis was performed on GC units and showed no specific clustering according to recording depth (PS vs non-PS, $k_{(15)} = 0.27$, $p = 0.22$; TS vs non-TS, $k_{(22)} = 0.18$, $p = 0.50$). In summary, response types appeared distributed equally along the extent of mPFC and GC, and no specific cluster of responses was identified.

Discussion

The gustatory portion of the insular cortex, commonly known as GC, is the most studied cortical recipient of taste information (Carleton et al., 2010; Maffei et al., 2012). However, GC is not the only cortical area involved in processing taste. Gustatory signals reach also the OFC and the mPFC (Gabbott et al., 2003; Gutierrez et al., 2006). Although considerable work has been devoted to understanding OFC contribution to taste processing, much less is known about mPFC involvement. Here we report evidence from electrophysiological recordings in alert rats demonstrating mPFC involvement in taste processing. Analysis of firing responses revealed similarities and differences in how taste engages neurons in mPFC and GC. Neurons in mPFC, like those in GC, can effectively process both taste quality and palatability. In both areas, some neurons encoded selectively for taste delivery (regardless of taste identity), taste quality, or taste palatability, whereas others showed mixed selectivity (Rigotti et al., 2013). mPFC and GC also shared a similarity in the temporal sequence of information processing, with taste identity being encoded first, followed by encoding of palatability. However, significant differences were also found. First, gustatory stimuli result in stronger and more widespread activation of GC than mPFC. Second, coding of taste quality occurs more rapidly in GC. Third, although palatability is coded equally well in GC and mPFC, neurons in mPFC show bias to aversive stimuli, which evoke stronger and more persistent responses than palatable tastants. Altogether, these differences suggest a division of labor among cortical areas involved in taste processing, with GC processing taste earlier than mPFC, and mPFC retaining longer palatability-related representations.

Taste coding in mPFC

The mPFC has been historically considered an area involved in cognitive and motivational control of behavior (Laubach, 2011). Behavioral tasks designed to investigate mPFC function have revealed, among others, responses to primary reinforcers, either positive or negative outcomes (Baeg et al., 2001; Matsumoto et al., 2003; Zhang et al., 2004; Horst and Laubach, 2013). Neurons in mPFC respond to rewards of different nature and magnitude. Fruit juice, different amounts of S, as well as rewarding intracranial stimulation have all been described to be effective in modulating activity in mPFC (Takenouchi et al., 1999; Amiez et al., 2006; Petykó et al., 2009). Although these studies demonstrated that outcome-related information can reach mPFC, to our knowledge, no experiment has been directed at understanding how mPFC neurons encode the different sensory qualities of natural rewards. Here we studied how mPFC responds to gustatory stimuli that differ for their sensory identity and their palatability, by passively administering tasting solutions via IOCs. Because responses in mPFC are known to be highly task dependent (Laubach, 2011), we chose to use an experimenter-controlled delivery paradigm (Katz et al., 2001; Fontanini and Katz, 2006). Such a design allowed us to focus on stimulus processing alone without engaging cognitive processes in the context of more complex behavioral tasks. The ability to respond to taste and encode gustatory information was evaluated in comparison with the GC, the primary cortical area devoted to process gustatory signals. Almost half of the neurons recorded in mPFC had their firing rates modulated by intraoral delivery of tasting solutions. However, tastants engaged mPFC less potently than GC. We found that a significantly lower percentage of mPFC responded to taste stimulation compared with GC. Furthermore, the magnitude of excitatory responses to tastants was smaller in mPFC than GC. Analysis of the taste coding in mPFC revealed that a significant number of prefrontal neurons can also respond specifically to different tastants. Several differences were observed in the ability of mPFC and GC neurons to encode taste. A lower number of mPFC neurons showed taste-selective responses compared with GC. Responses to tastants appeared to be sparser and more narrowly tuned in mPFC compared with GC. The majority of mPFC neurons responded to one or two tastants. Conversely, in GC, the majority of neurons were broadly tuned and responded selectively to three or four stimuli. A comparative analysis of taste coding indicated a better

classification performance for gustatory cortical neurons compared with prefrontal ones. Single neurons as well as pseudo-ensembles of neurons in mPFC contained less taste-related information than in GC yet were capable of allowing significantly above-chance taste classification. Decoding analysis on a surrogate dataset based on mPFC neurons revealed that >95% accurate classification performance could be achieved with as little as 300 mPFC neurons.

We cannot definitively exclude that the taste coding activity observed in mPFC might be related, at least in part, to different consummatory behaviors triggered by specific tastants. However, EMG recordings performed in experimental conditions similar to ours (Travers and Norgren, 1986) revealed that taste-selective orofacial reactions occur at a latency longer than 1 s. We computed the latency of identity coding with different methods and found that it was consistently faster than 1 s, suggesting that at least the early portion of the taste specificity observed is not attributable to taste-specific mouth movements.

Although mPFC encoded taste quality less successfully than GC, it was at least as good as GC in encoding palatability. A quarter of mPFC neurons produced responses that matched the hedonic value of the four tastants used. Although no specific pattern of firing to rewarding and aversive tastants was observed in excitatory and inhibitory responses in GC, mPFC consistently responded more strongly to aversive gustatory stimuli. Q and C resulted in stronger excitation or stronger inhibition than S and N. These results suggest a bias for aversive gustatory stimuli in the population of mPFC palatability-specific neurons. Interestingly, palatability coding persisted longer in mPFC than in GC. Presence of persistent responses to hedonic value are consistent with evidence showing persistent activity in mPFC (Baeg et al., 2001, 2003; Narayanan and Laubach, 2008, 2009).

Although the latency for palatability coding is shorter than the one reported for orofacial reactions (Travers and Norgren, 1986), the persistence of the bias toward aversive tastants observed in mPFC could potentially be related to differences in how the rats consumed rewarding and aversive solutions. Tongue protrusions and gapes might also contribute to this bias, as also suggested by recent reports showing a close relationship between mPFC activity and licking behavior (Horst and Laubach, 2013). However, whether mouth movements would be the cause or the effect of the persistent differential activity in mPFC is not known. Future studies combining electrophysiological recordings, EMG recordings, and video analysis will be directed at investigating this issue in depth. Regardless of the potential coupling between sensorimotor behaviors and mPFC bias toward aversive stimuli, we note that such a bias was not observed in GC, another area in which long-latency firing could also in principle be modulated by ingestive behaviors. This result further emphasizes the functional differences between mPFC and GC.

GC–mPFC flow of gustatory information

The mPFC receives dense projections from the gustatory and visceral portions of the insular cortex (Gabbott et al., 2003). To our knowledge, projections to mPFC from other gustatory areas are limited. Tracing experiments have shown that the parvicellular portion of the ventroposteromedial nucleus of the thalamus, the thalamic source of gustatory signals to GC, does not project directly to mPFC (Condé et al., 1990). Similarly, projections from the parabrachial nucleus to mPFC are lighter than those to GC and unlikely to be a significant source of gustatory information (Divac et al., 1978; Saper and Loewy, 1980). Hence, processing of gustatory quality in mPFC is likely dependent on inputs from GC. If that is the case, one should expect gustatory responses to have a faster onset in GC than in mPFC. Indeed, our data show a faster onset of taste identity coding in GC relative to mPFC. Although these results are not sufficient to draw a causal relationship between activity in GC and activity in mPFC, they are consistent with a model in which gustatory signals activate serially GC and then mPFC. The observation that fewer mPFC neurons are activated by taste indicates a loss in the transmission of gustatory signals from GC to mPFC. Signals are also transformed, as neurons become less broadly tuned and representations are sparser in mPFC. This result is consistent with the view that mPFC cortex represents a higher-order area involved in integrating taste with multiple other stimuli.

As for the sources of hedonic coding, those can be numerous. Areas such as the amygdala, the mediodorsal thalamus, and the lateral hypothalamus are known to be involved in processing rewarding and hedonic value (Oyoshi et al., 1996; Fontanini et al., 2009; Li et al., 2013; Zhang et al., 2013) and are known to send significant projections to mPFC (Hoover and Vertes, 2007). The GC itself shows neurons whose responsiveness is primarily influenced by the palatability (Fontanini and Katz, 2006; Grossman et al., 2008). Consistently, GC could also be one of the sources of hedonic signals to mPFC. In general accordance with previous reports, palatability-related activity in GC starts at around ~0.75 s (Sadacca et al., 2012). The overall onset of palatability responses is similar in GC and mPFC. However, palatability-related activity had a different duration in the two areas, lasting longer in mPFC than GC. Our data are compatible with the view that palatability signals from different sources, including GC, could converge in mPFC and generate sustained activity.

Although our data are consistent with gustatory signals traveling from GC to mPFC, anatomical reports also show evidence of reciprocal projection between the two areas (Gabbott et al., 2003). A recent model has suggested that bidirectional connections between GC and mPFC might play a role generating persistent activity (Laubach, 2011). Evidence of persistent hedonic signals in mPFC is consistent with this view. However, more experiments are needed to investigate the function of reciprocal connections and the nature of the information passed from mPFC to GC.

Gustatory coding and current views of mPFC

The mPFC has been investigated intensely for its role in controlling motivated behaviors (Wallis and Kennerley, 2010; Laubach, 2011; Kvitsiani et al., 2013). Recordings from an array of behavioral paradigms have shown that neurons in mPFC change their firing rates in relation to multiple cognitive processes. Strong evidence has also been accumulating on the involvement of mPFC in encoding predictive cues and behavioral outcomes (Matsumoto et al., 2003; Amiez et al., 2006; Bouret and Richmond, 2010; Wallis and Kennerley, 2010). It is well known that activity in mPFC can be strongly modulated by natural rewards, such as sucrose, juice, or food. Neurons in mPFC do not just respond to rewarding stimuli, they can also signal aversive events (Baeg et al., 2001; Zhang et al., 2013). mPFC can retain persistent representations of negative outcomes, such as errors in performing a task (Narayanan and Laubach, 2008). Neurons in the mPFC can also persistently encode nociceptive stimulation (Zhang et al., 2004; Onozawa et al., 2011) and respond to cues anticipating noxious stimulus with responses lasting several seconds (Baeg et al., 2001). In addition, it has been reported that mPFC plays a role in the formation and retrieval of aversive taste memories (Hernádi et al., 2000). Our results confirm mPFC involvement in

processing aversive events and further show that aversive gustatory stimuli appear particularly effective in activating a subset of taste-specific neurons. In particular, we found that aversive gustatory stimuli evoke stronger and longer-lasting responses than rewarding stimuli in neurons tuned to encode hedonic value. Although these data are not evidence for a generalized tuning of mPFC toward aversive events, they nevertheless suggest that, when it comes to taste, mPFC neurons appear more sensitive to unpalatable tastants than to palatable ones.

It is important to notice that representations of positive and negative outcomes in mPFC are not abstract and stimulus independent. In fact, the data presented here indicate that mPFC can effectively encode not only the hedonic value of a tasting solution but also its specific sensory identity. The ability to finely represent different gustatory qualities, i.e., sweet, salty, sour, and bitter, is consistent with an involvement of mPFC in selecting appropriate nutrients and avoiding specific substances (Nagy et al., 2012; Horst and Laubach, 2013). These results, together with evidence showing that neurons in mPFC can encode homeostatic signals and drive licking (Horst and Laubach, 2013), suggest a fundamental involvement of this area in adaptively regulating feeding behaviors.

References

Accolla R, Carleton A (2008) Internal body state influences topographical plasticity of sensory representations in the rat gustatory cortex. Proc Natl Acad Sci U S A 105:4010–4015. CrossRef Medline

Amiez C, Joseph JP, Procyk E (2006) Reward encoding in the monkey anterior cingulate cortex. Cereb Cortex 16:1040–1055. CrossRef Medline

Baeg EH, Kim YB, Jang J, Kim HT, Mook-Jung I, Jung MW (2001) Fast spiking and regular spiking neural correlates of fear conditioning in the medial prefrontal cortex of the rat. Cereb Cortex 11:441–451. CrossRef Medline

Baeg EH, Kim YB, Huh K, Mook-Jung I, Kim HT, Jung MW (2003) Dynamics of population code for working memory in the prefrontal cortex. Neuron 40:177–188. CrossRef Medline

Baylis LL, Rolls ET, Baylis GC (1995) Afferent connections of the caudolateral orbitofrontal cortex taste area of the primate. Neuroscience 64:801–812. CrossRef Medline

Benjamini Y, Hochberg Y (1995) Controlling the false discovery rate: a practical and powerful approach to multiple testing. J R Stat Soc B 57:289–300.

Bouret S, Richmond BJ (2010) Ventromedial and orbital prefrontal neurons differentially encode internally and externally driven motivational values in monkeys. J Neurosci 30:8591–8601. CrossRef Medline

Carleton A, Accolla R, Simon SA (2010) Coding in the mammalian gustatory system. Trends Neurosci 33:326–334. CrossRef Medline

Cohen JY, Haesler S, Vong L, Lowell BB, Uchida N (2012) Neuron-type-specific signals for reward and punishment in the ventral tegmental area. Nature 482:85–88. CrossRef Medline

Condé F, Audinat E, Maire-Lepoivre E, Crépel F (1990) Afferent connections of the medial frontal cortex of the rat. A study using retrograde transport of fluorescent dyes. I. Thalamic afferents. Brain Res Bull 24:341–354. CrossRef Medline

Di Lorenzo PM, Chen JY, Victor JD (2009) Quality time: representation of a multidimensional sensory domain through temporal coding. J Neurosci 29:9227–9238. CrossRef Medline

DiMatteo I, Genovese CR, Kass RE (2001) Bayesian curve-fitting with free-knot splines. Biometrika 88:1055–1071. CrossRef

Divac I, Kosmal A, Björklund A, Lindvall O (1978) Subcortical projections to the prefrontal cortex in the rat as revealed by the horseradish peroxidase technique. Neuroscience 3:785–796. CrossRef Medline

Efron B (1986) Jackknife, bootstrap and other resampling methods in regression-analysis: discussion. Ann Stat 14:1301–1304. CrossRef

Fontanini A, Katz DB (2006) State-dependent modulation of time-varying gustatory responses. J Neurophysiol 96:3183–3193. CrossRef Medline

Fontanini A, Katz DB (2008) Behavioral states, network states, and sensory response variability. J Neurophysiol 100:1160–1168. CrossRef Medline

Fontanini A, Grossman SE, Figueroa JA, Katz DB (2009) Distinct subtypes of basolateral amygdala taste neurons reflect palatability and reward. J Neurosci 29:2486–2495. CrossRef Medline

Gabbott PL, Warner TA, Jays PR, Bacon SJ (2003) Areal and synaptic interconnectivity of prelimbic (area 32), infralimbic (area 25) and insular cortices in the rat. Brain Res 993:59–71. CrossRef Medline

Gallistel CR, Fairhurst S, Balsam P (2004) The learning curve: implications of a quantitative analysis. Proc Natl Acad Sci U S A 101:13124–13131. CrossRef Medline

Grossman SE, Fontanini A, Wieskopf JS, Katz DB (2008) Learning-related plasticity of temporal coding in simultaneously recorded amygdala-cortical ensembles. J Neurosci 28:2864–2873. CrossRef Medline

Gutierrez R, Carmena JM, Nicolelis MA, Simon SA (2006) Orbitofrontal ensemble activity monitors licking and distinguishes among natural rewards. J Neurophysiol 95:119–133. Medline

Gutierrez R, Simon SA, Nicolelis MA (2010) Licking-induced synchrony in the taste-reward circuit improves cue discrimination during learning. J Neurosci 30:287–303. CrossRef Medline

Hernádi I, Karádi Z, Vígh J, Petykó Z, Egyed R, Berta B, Lénárd L (2000) Alterations of conditioned taste aversion after microiontophoretically applied neurotoxins in the medial prefrontal cortex of the rat. Brain Res Bull 53:751–758. CrossRef Medline

Hoover WB, Vertes RP (2007) Anatomical analysis of afferent projections to the medial prefrontal cortex in the rat. Brain Struct Funct 212:149–179. CrossRef Medline

Horst NK, Laubach M (2013) Reward-related activity in the medial prefrontal cortex is driven by consumption. Front Neurosci 7:56. CrossRef Medline

Jezzini A, Caruana F, Stoianov I, Gallese V, Rizzolatti G (2012) Functional organization of the insula and inner perisylvian regions. Proc Natl Acad Sci U S A 109:10077–10082. CrossRef Medline

Kadohisa M, Rolls ET, Verhagen JV (2005) Neuronal representations of stimuli in the mouth: the primate insular taste cortex, orbitofrontal cortex and amygdala. Chem Senses 30:401–419. CrossRef Medline

Katz DB (2005) The many flavors of temporal coding in gustatory cortex. Chem Senses 30 [Suppl 1]:i80–i81. CrossRef

Katz DB, Simon SA, Nicolelis MA (2001) Dynamic and multimodal responses of gustatory cortical neurons in awake rats. J Neurosci 21:4478–4489. Medline

Katz DB, Nicolelis MA, Simon SA (2002) Gustatory processing is dynamic and distributed. Curr Opin Neurobiol 12:448–454. CrossRef Medline

Kvitsiani D, Ranade S, Hangya B, Taniguchi H, Huang JZ, Kepecs A (2013) Distinct behavioural and network correlates of two interneuron types in prefrontal cortex. Nature 498:363–366. CrossRef Medline

La Camera G, Richmond BJ (2008) Modeling the violation of reward maximization and invariance in reinforcement schedules. PLoS Comput Biol 4:e1000131. CrossRef Medline

La Camera G, Rauch A, Thurbon D, Lüscher HR, Senn W, Fusi S (2006) Multiple time scales of temporal response in pyramidal and fast spiking cortical neurons. J Neurophysiol 96:3448–3464. CrossRef Medline

Laubach M (2011) A comparative perspective on executive and motivational control by the medial prefrontal cortex. In: Neural basis of motivational and cognitive control (Mars RB, Sallet J, Rushworth MFS, Yeung N, eds). Cambridge, MA: Massachusetts Institute of Technology.

Li JX, Yoshida T, Monk KJ, Katz DB (2013) Lateral hypothalamus contains two types of palatability-related taste responses with distinct dynamics. J Neurosci 33:9462–9473. CrossRef Medline

Maffei A, Haley M, Fontanini A (2012) Neural processing of gustatory information in insular circuits. Curr Opin Neurobiol 22:709–716. CrossRef Medline

Maier JX, Katz DB (2013) Neural dynamics in response to binary taste mixtures. J Neurophysiol 109:2108–2117. CrossRef Medline

Matsumoto K, Suzuki W, Tanaka K (2003) Neuronal correlates of goal-based motor selection in the prefrontal cortex. Science 301:229–232. CrossRef Medline

Minamimoto T, La Camera G, Richmond BJ (2009) Measuring and modeling the interaction among reward size, delay to reward, and satiation level on motivation in monkeys. J Neurophysiol 101:437–447. CrossRef Medline

Nagy B, Szabó I, Papp S, Takács G, Szalay C, Karádi Z (2012) Glucose-monitoring neurons in the mediodorsal prefrontal cortex. Brain Res 1444:38–44. CrossRef Medline

Narayanan NS, Laubach M (2008) Neuronal correlates of post-error slow-

ing in the rat dorsomedial prefrontal cortex. J Neurophysiol 100:520–525. CrossRef Medline

Narayanan NS, Laubach M (2009) Delay activity in rodent frontal cortex during a simple reaction time task. J Neurophysiol 101:2859–2871. CrossRef Medline

Onozawa K, Yagasaki Y, Izawa Y, Abe H, Kawakami Y (2011) Amygdala-prefrontal pathways and the dopamine system affect nociceptive responses in the prefrontal cortex. BMC Neurosci 12:115. CrossRef Medline

Oyoshi T, Nishijo H, Asakura T, Takamura Y, Ono T (1996) Emotional and behavioral correlates of mediodorsal thalamic neurons during associative learning in rats. J Neurosci 16:5812–5829. Medline

Petykó Z, Tóth A, Szabó I, Gálosi R, Lénárd L (2009) Neuronal activity in rat medial prefrontal cortex during sucrose solution intake. Neuroreport 20: 1235–1239. CrossRef Medline

Phillips MI, Norgren R (1970) A rapid method for permanent implantation of an intraoral fistula in rats. Behav Res Methods Instrum Comput 1:124–126.

Piette CE, Baez-Santiago MA, Reid EE, Katz DB, Moran A (2012) Inactivation of basolateral amygdala specifically eliminates palatability-related information in cortical sensory responses. J Neurosci 32:9981–9991. CrossRef Medline

Press WH, Teukolsky SA, Vetterling WT, Flannery BP (2007) Numerical recipes the art of scientific computing, Ed 3, Online resource (xxi, 1235 p. ill, 1227 cm). Cambridge, UK: Cambridge UP.

Rigotti M, Barak O, Warden MR, Wang XJ, Daw ND, Miller EK, Fusi S (2013) The importance of mixed selectivity in complex cognitive tasks. Nature 497:585–590. CrossRef Medline

Sadacca BF, Rothwax JT, Katz DB (2012) Sodium concentration coding gives way to evaluative coding in cortex and amygdala. J Neurosci 32: 9999–10011. CrossRef Medline

Samuelsen CL, Gardner MP, Fontanini A (2012) Effects of cue-triggered expectation on cortical processing of taste. Neuron 74:410–422. CrossRef Medline

Samuelsen CL, Gardner MP, Fontanini A (2013) Thalamic contribution to cortical processing of taste and expectation. J Neurosci 33:1815–1827. CrossRef Medline

Saper CB, Loewy AD (1980) Efferent connections of the parabrachial nucleus in the rat. Brain Res 197:291–317. CrossRef Medline

Shao J (1993) Linear-model selection by cross-validation. J Am Stat Assoc 88:486–494. CrossRef

Small DM, Bender G, Veldhuizen MG, Rudenga K, Nachtigal D, Felsted J (2007) The role of the human orbitofrontal cortex in taste and flavor processing. Ann N Y Acad Sci 1121:136–151. CrossRef Medline

Spector AC, Travers SP (2005) The representation of taste quality in the mammalian nervous system. Behav Cogn Neurosci Rev 4:143–191. CrossRef Medline

Stapleton JR, Lavine ML, Nicolelis MA, Simon SA (2007) Ensembles of gustatory cortical neurons anticipate and discriminate between tastants in a single lick. Front Neurosci 1:161–174. CrossRef Medline

Stone M (1974) Cross-validatory choice and assessment of statistical predictions. J R Stat Soc B 36:111–147.

Takenouchi K, Nishijo H, Uwano T, Tamura R, Takigawa M, Ono T (1999) Emotional and behavioral correlates of the anterior cingulate cortex during associative learning in rats. Neuroscience 93:1271–1287. CrossRef Medline

Travers JB, Norgren R (1986) Electromyographic analysis of the ingestion and rejection of sapid stimuli in the rat. Behav Neurosci 100:544–555. CrossRef Medline

Verhagen JV, Giza BK, Scott TR (2003) Responses to taste stimulation in the ventroposteromedial nucleus of the thalamus in rats. J Neurophysiol 89: 265–275. Medline

Wallis JD, Kennerley SW (2010) Heterogeneous reward signals in prefrontal cortex. Curr Opin Neurobiol 20:191–198. CrossRef Medline

Yamamoto T, Yuyama N, Kato T, Kawamura Y (1985) Gustatory responses of cortical neurons in rats. II. Information processing of taste quality. J Neurophysiol 53:1356–1369. Medline

Zhang R, Tomida M, Katayama Y, Kawakami Y (2004) Response durations encode nociceptive stimulus intensity in the rat medial prefrontal cortex. Neuroscience 125:777–785. CrossRef Medline

Zhang W, Schneider DM, Belova MA, Morrison SE, Paton JJ, Salzman CD (2013) Functional circuits and anatomical distribution of response properties in the primate amygdala. J Neurosci 33:722–733. CrossRef Medline